

## Direct observation of half-metallic energy gap in Co<sub>2</sub>MnSi by tunneling conductance spectroscopy

Y. Sakuraba,<sup>a)</sup> T. Miyakoshi, M. Oogane, Y. Ando, A. Sakuma, and T. Miyazaki  
 Department of Applied Physics, Graduate School of Engineering, Tohoku University, Aoba-yama 6-6-05,  
 Aramaki, Aoba-ku, Sendai 980-8579, Japan

H. Kubota

Nanoelectronics Research Institute, National Institute of Advanced Industrial Science and Technology  
 (AIST), 1-1-1 Umezono, Tsukuba 305-8568, Japan

(Received 26 April 2006; accepted 24 June 2006; published online 3 August 2006)

Magnetic tunnel junctions with a Co<sub>2</sub>MnSi/Al–O/CoFe structure are prepared by magnetron sputtering and investigated with respect to the energy gap near the Fermi energy level. The plasma oxidation time for the Al–O barrier is found to affect the condition of the Co<sub>2</sub>MnSi/Al–O interface. The optimized sample (50 s oxidation time) exhibits a magnetoresistance ratio of 159% and tunneling spin polarization of 0.89 at 2 K. The bias voltage dependence of tunneling conductance ( $dI/dV$ – $V$ ) reveals a clear half-metallic energy gap at 350–400 meV for Co<sub>2</sub>MnSi, with an energy separation of just 10 meV between the Fermi energy and the bottom edge of conduction band.

© 2006 American Institute of Physics. [DOI: 10.1063/1.2335583]

One of the most interesting and attractive goals of spintronics is the fabrication of an ideal half-metallic material (HMF) capable of large tunneling magnetoresistance (TMR) and giant magnetoresistance at room temperature (RT). Previous theoretical works have predicted that certain oxides (La<sub>2/3</sub>Sr<sub>1/3</sub>MnO<sub>3</sub>, CrO<sub>2</sub>, Fe<sub>3</sub>O<sub>4</sub>),<sup>1–3</sup> zinc-blend-type compounds (CrAs, CrSb, etc.),<sup>4,5</sup> and Heusler alloys (NiMnSb, Co<sub>2</sub>MnSi, Co<sub>2</sub>MnGe, Co<sub>2</sub>CrAl, etc.)<sup>6–8</sup> are capable of half-metallic band structures. Among these candidates for HMFs, the full-Heusler alloy Co<sub>2</sub>MnSi (CMS) is the most promising material for realizing half-metallicity at RT due to its high Curie temperature of 985 K. The present authors recently fabricated magnetic tunnel junctions (MTJs) with a Co<sub>2</sub>MnSi/Al–O/Co<sub>75</sub>Fe<sub>25</sub> structure using a magnetron sputtering system.<sup>9</sup> The observed MR ratio of 159% and tunneling spin polarization of 0.89 at 2 K suggest that CMS exhibits its half-metallic properties. In that study, however, all MR measurements were conducted at low bias voltage (1 mV). Thus, there have been no direct observations of the half-metallic energy gap with respect to the applied bias voltage.

In the simple model of a MTJ,<sup>10</sup> the tunneling conductance  $dI/dV$  is proportional to  $D_M^L D_M^R + D_m^L D_m^R$  in the parallel configuration and to  $D_M^L D_m^R + D_m^L D_M^R$  in the antiparallel configuration, where each term represents the density of states  $D$  at the  $E_F$  for the majority ( $M$ ) or minority ( $m$ ) spins of the left ( $L$ ) or right ( $R$ ) electrode. Information regarding the density of states (DOS) around the  $E_F$  can therefore be extracted from the shape of the  $dI/dV$ – $V$  curve. Previous investigation on tunneling conductance for MTJ using La<sub>2/3</sub>Sr<sub>1/3</sub>MnO<sub>3</sub> clearly reveals the gap of 0.34 eV between  $E_F$  and the bottom the minority-spin band, which is quite consistent with the result of spin-polarized inverse photoemission measurements.<sup>11</sup>

The purpose of the present study is to observe the half-metallic energy gap of CMS directly by measuring the  $dI/dV$ – $V$  curve of a Co<sub>2</sub>MnSi/Al–O/CoFe MTJ at low temperature. The half-metallic energy gap ( $E_G$ ) of CMS has been

predicted to be approximately 0.4–0.6 eV,<sup>6</sup> which is far below the static breakdown voltage of Al–O insulating barriers. A number of MTJs are prepared to examine the effect of Al–O barrier oxidation time on the interface structure and energy gap.

The devices, with structure of MgO(100) substrate/epitaxial Cr (40 nm)/epitaxial Co<sub>2</sub>MnSi (30 nm)/Al–O (1.3 nm)/Co<sub>75</sub>Fe<sub>25</sub> (5 nm)/Ir<sub>22</sub>Mn<sub>78</sub> (10 nm)/Ta (3 nm), were prepared using an ultrahigh vacuum magnetron sputtering system. The (100)-oriented epitaxial CMS bottom electrode was grown at ambient temperature followed by annealing at 450 °C to improve the order of the  $L2_1$  crystal structure. A composition-adjusted CMS alloy sputtering target (Co, 43.7%; Mn, 27.95%; Si, 28.35%) was used to produce a stoichiometric film composition. The Al–O tunnel barrier was formed by plasma oxidation of a predeposited 1.3-nm-thick Al layer. The plasma oxidation time  $t_{ox}$  was varied from 10 to 240 s to examine the influence on interface quality. The MTJ films were patterned into  $10 \times 10$ – $100 \times 100 \mu\text{m}^2$  elements by photolithography combined with Ar ion and CHF<sub>3</sub> reactive ion etching. After microfabrication, MTJs were annealed under a high vacuum and an external magnetic field of 300 Oe. MR measurements were performed using a standard dc four-probe method, and the dependence of the tunneling conductance on bias voltage ( $dI/dV$ – $V$ ) was measured at 10 K using an ac lock-in technique. A positive bias voltage is defined as electrons tunneling from the lower Co<sub>2</sub>MnSi to the upper Co<sub>75</sub>Fe<sub>25</sub> electrode.

The  $t_{ox}$  dependence of resistance area (RA) products is shown in Fig. 1(a). The result for Co<sub>75</sub>Fe<sub>25</sub>/Al–O/Co<sub>75</sub>Fe<sub>25</sub> is also shown for reference. The RA values for CMS/Al–O/Co<sub>75</sub>Fe<sub>25</sub> changed systematically with increasing  $t_{ox}$ , saturating at ca.  $10^7 \Omega \mu\text{m}^2$  as  $t_{ox}$  exceeded 180 s. The RA values for CMS/Al–O/Co<sub>75</sub>Fe<sub>25</sub> are approximately one order of magnitude larger than those for Co<sub>75</sub>Fe<sub>25</sub>/Al–O/Co<sub>75</sub>Fe<sub>25</sub> over the entire range of  $t_{ox}$ , despite the oxidation condition of the tunnel barrier layer in the sputtering device being unchanged. Such an elevation of RA values was also observed in the previous study for MTJs

<sup>a)</sup>Electronic mail: sakuraba@mlab.apph.tohoku.ac.jp

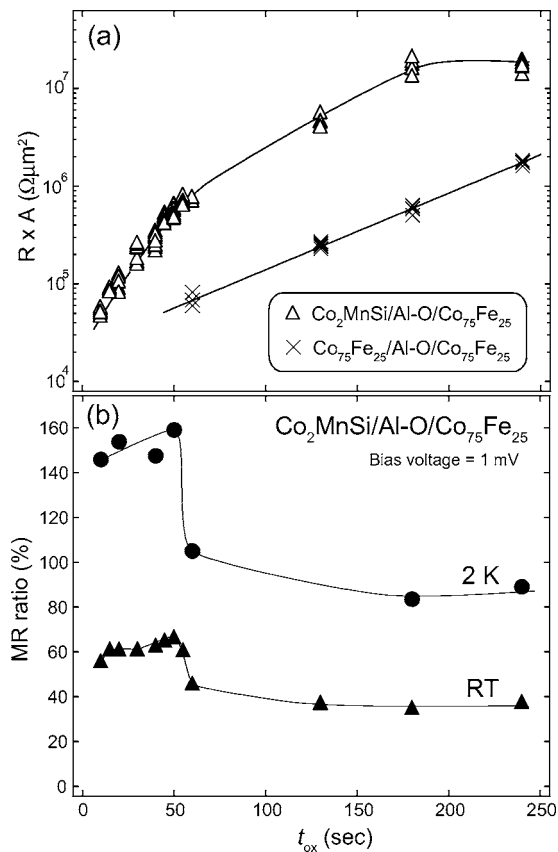


FIG. 1. (Color online) Dependence of (a) resistance area (RA) product and (b) MR ratio on plasma oxidation time ( $t_{\text{ox}}$ ) for MTJs prepared with an epitaxial CMS bottom electrode and a conventional  $\text{Co}_{75}\text{Fe}_{25}$  electrode.

fabricated with  $\text{Co}_2\text{MnAl}$  bottom electrodes.<sup>12</sup> The maximum MR ratio achieved after annealing is plotted as a function of plasma oxidation time  $t_{\text{ox}}$  in Fig. 1(b). High MR ratios exceeding 140% were observed at 2 K, even for MTJs fabricated with the shortest oxidation time ( $t_{\text{ox}}=10$  s). The MR ratio increased to 159% with increasing  $t_{\text{ox}}$  up to 50 s. Interestingly, the MR ratio then underwent a dramatic decrease to approximately 100% upon further oxidation ( $t_{\text{ox}} > 60$  s). This reduction of the MR ratio and elevation of RA values are considered to be due to the generation of oxides at the CMS/Al-O interface, since Mn and Si atoms have a strong affinity for oxygen compared to conventional ferromagnetic elements such as Fe and Co.<sup>13</sup> High-resolution transmission electron microscopy (HRTEM) images of the optimized MTJ ( $t_{\text{ox}}=50$  s) and an overoxidized MTJ ( $t_{\text{ox}}=240$  s) are shown in Fig. 2. Although extremely flat interfaces were observed near the Al-O barrier layer in both cases, a thin contaminant layer could be seen on the CMS surface in the overoxidized case. The Al-O barrier layer in the overoxidized case was also considerably thicker (3 nm) than the predeposited Al layer (1.3 nm). This contaminant layer at the CMS surface and thickening of the barrier are strongly suggestive of the generation of an oxidized layer at the CMS interface, resulting in the observed reduction in the MR ratio and larger RA value for the overoxidized MTJ (see Fig. 1).

The dependence of the conductance curves ( $dI/dV-V$ ) on bias voltage for the optimized MTJ ( $t_{\text{ox}}=50$  s) in the parallel magnetization configuration is shown in Fig. 3(a). The MTJs were annealed at temperatures ( $T_a$ ) of up to 350 °C. The dependence of the MR ratios on  $T_a$  is also shown. The

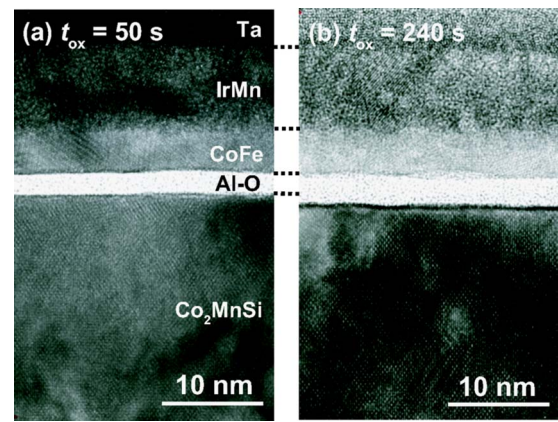


FIG. 2. (Color online) HRTEM images of (a) optimally oxidized ( $t_{\text{ox}}=50$  s) and (b) overoxidized ( $t_{\text{ox}}=180$  s) MTJs. Both MTJs were annealed at the temperature giving the highest TMR ratio.

parallel magnetization configuration is considered here in order to discuss the DOS around the Fermi level, as tunneling conductance in the antiparallel configuration is affected by the contribution of inelastic tunneling processes involving magnon excitation at low bias voltage. In the as-deposited state, the observed MR ratio was low (104% at 10 K), and the  $dI/dV-V$  curve was relatively symmetric with respect to the sign of the applied bias voltage. This symmetry is a general feature of conventional MTJs with CoFe or NiFe electrodes. Interestingly, this symmetric  $dI/dV-V$  curve gradually deforms to yield a gap structure at around +350 mV upon annealing at 200–300 °C. This behavior corresponds to an

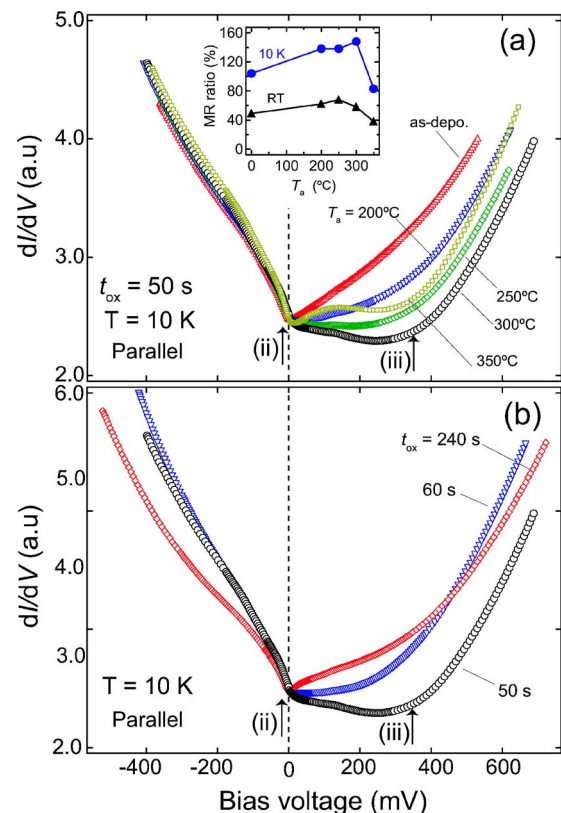


FIG. 3. (Color online) Dependence of tunneling conductance on bias voltage for  $\text{CMS}/\text{Al-O}/\text{Co}_{75}\text{Fe}_{25}$  MTJs under parallel magnetization at 10 K. (a) Variation of optimized MTJs with respect to annealing temperature  $T_a$  (change in MR ratio inset). (b) Variation of MTJs prepared with various oxidation times.

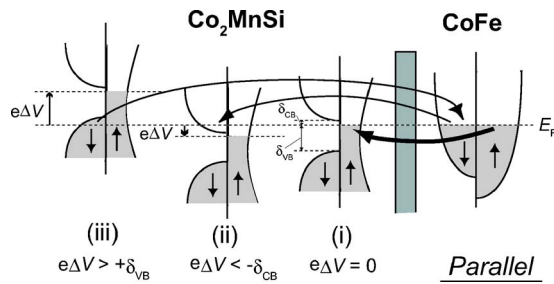


FIG. 4. (Color online) Schematic of electron tunneling processes at finite bias voltages in the CMS/Al-O/Co<sub>75</sub>Fe<sub>25</sub> system under parallel magnetization.

increase in the MR ratio (see inset). The gap structure at around +350 mV degrades upon annealing at 350 °C, corresponding to a dramatic decrease in the MR ratio. The  $dI/dV-V$  curves for MTJs prepared with different  $t_{\text{ox}}$  times (50, 60, and 240 s) are shown in Fig. 3(b) for comparison. Each MTJ was annealed at the temperature giving the maximum MR ratio. The MTJ with  $t_{\text{ox}}=50$  s displayed the highest TMR ratio of 159% at 2 K, whereas the overoxidized MTJs ( $t_{\text{ox}}=60$ , and 240 s) exhibited much lower TMR ratios (105% and 89%), as shown in Fig. 1(b). The gap structure at around +350 mV and the asymmetry of the  $dI/dV-V$  curve became remarkable in MTJs having higher MR ratios. We note here that these asymmetric  $dI/dV-V$  curves were not attributed to the simple asymmetry of tunneling barrier height because barrier asymmetry should become large in overoxidized MTJ having large difference of interfacial conditions between upper and lower sides of Al-O barrier. In addition, the theoretical model of Brinkman *et al.* regarding barrier asymmetry cannot fit the shape of our asymmetric  $dI/dV-V$  curves well.<sup>14</sup> Therefore we can consider the shapes of  $dI/dV-V$  curves reflect the band structure of CMS as follows.

The relationship between the observed bias voltage dependence of  $dI/dV$  and the half-metallic band structure of CMS is shown in Fig. 4 in terms of the electron tunneling processes at finite bias voltages in the parallel configuration. For simplicity, the ideal half-metallic DOS is assumed for the CMS bottom electrode. The energy separation between the Fermi level and the bottom of the conduction band (or top of the valence band) in the minority-spin band of CMS is represented by  $\delta_{\text{CB}}$  (or  $\delta_{\text{VB}}$ ). At the low bias limit [see in Fig. 4(i)], tunneling conductance is dominated by majority-majority electron tunneling, which is proportional to  $D_M^{\text{CMS}}(E_F)D_M^{\text{CoFe}}(E_F)$ . When the applied bias voltage ( $\Delta V$ ) becomes equivalent to  $-\delta_{\text{CB}}/e$  or  $+\delta_{\text{VB}}/e$ , the minority-minority tunneling channels open, as shown in Figs. 4(ii) and 4(iii). The rapid increase in  $dI/dV$  at low negative biases (ca. -10 mV) in Fig. 3(a) is due to the creation of a minority-minority tunneling channel derived from the bottom edge of the conduction band. The rapid increase in  $dI/dV$  seen in Fig. 3(a) is similarly due to a minority-minority channel derived from the top edge of the valence band at around +350 mV. The values of  $\delta_{\text{CB}}$  (10–20 meV) and  $\delta_{\text{VB}}$  (350–400 meV) obtained from these results are in good agreement with theoretical calculations and previous  $dI/dV-V$  measurements using Co<sub>2</sub>MnSi/Al-O/Co<sub>2</sub>MnSi MTJ.<sup>6,15</sup>

In summary, MTJs with a Co<sub>2</sub>MnSi/Al-O/CoFe structure were fabricated, and the influence of Al-O barrier oxidation time on the CMS/Al-O interface condition and energy gap of the MTJ was examined. In the range of  $t_{\text{ox}}$  investigated (10–240 s), the device prepared with  $t_{\text{ox}}=50$  s exhibited the highest MR ratio (159%) and tunneling spin polarization (0.89) at 2 K. The bias voltage dependence of the tunneling conductance ( $dI/dV-V$ ) revealed a clear half-metallic energy gap at 350–400 meV for CMS, where an energy separation of 10 meV was observed between the Fermi energy and the bottom edge of the conduction band ( $\delta_{\text{CB}}$ ). This is the first clear experimental evidence of the half-metallic gap structure of CMS. The small  $\delta_{\text{CB}}$  value of 10 meV derived in the present study may be one reason for the large temperature dependence of the TMR ratio, as the inferred thermal fluctuation energy at RT is approximately 30 meV. This can be compared to the large  $\delta_{\text{CB}}$  (i.e., energy separation from  $E_F$  to minority  $\Delta_1$  band edge) of 1.2 eV reported for a Fe/MgO/Fe MTJ.<sup>16,17</sup> Further experiments examining the possibility of shifting  $E_F$  to the center of the half-metallic energy gap should be conducted in order to realize higher TMR ratios at RT for CMS-based MTJs.

This study was supported by the IT Program of the Research Revolution 2002 (RR2002) under the title “Development of Universal Low-Power Spin Memory,” by a Grant-in-Aid for Scientific Research from the Ministry of Education, Culture, Sports, Science and Technology of Japan, by the Core Research for Evolutional Science and Technology (CREST) program of the Japan Science and Technology (JST) Corporation, by the Grant Program of the New Energy and Industrial Development Organization (NEDO), and by a Research Fellowship for Young Scientists from the Japan Society for the Promotion of Science (JSPS).

<sup>1</sup>S. Lewis, P. Allen, and T. Sasaki, Phys. Rev. B **55**, 10253 (1997).

<sup>2</sup>Z. Zhang and S. Satpathi, Phys. Rev. B **44**, 13319 (1991).

<sup>3</sup>W. Pickett and D. Singh, Phys. Rev. B **53**, 1146 (1996).

<sup>4</sup>M. Shirai, T. Ogawa, I. Kitagawa, and N. Suzuki, J. Magn. Magn. Mater. **177–181**, 1383 (1998).

<sup>5</sup>H. Akinaga, T. Manago, and M. Shirai, Jpn. J. Appl. Phys., Part 2 **39**, L1118 (2000).

<sup>6</sup>S. Ishida, S. Fujii, S. Kashiwagi, and S. Asano, J. Phys. Soc. Jpn. **64**, 2152 (1995).

<sup>7</sup>I. Galanakis, P. H. Dederichs, and N. Papanikolaou, Phys. Rev. B **66**, 174429 (2002).

<sup>8</sup>I. Galanakis, P. H. Dederichs, and N. Papanikolaou, Phys. Rev. B **66**, 134428 (2002).

<sup>9</sup>Y. Sakuraba, J. Nakata, M. Oogane, H. Kubota, Y. Ando, A. Sakuma, and T. Miyazaki, Jpn. J. Appl. Phys., Part 2 **44**, L1100 (2005).

<sup>10</sup>M. Julliere, Phys. Lett. **54A**, 225 (1975).

<sup>11</sup>M. Bowen, A. Barthélémy, M. Bibes, E. Jacquet, J.-P. Contour, A. Fert, F. Ciccacci, L. Duó and R. Bertacco, Phys. Rev. Lett. **95**, 137203 (2005).

<sup>12</sup>Y. Sakuraba, J. Nakata, M. Oogane, H. Kubota, Y. Ando, H. Kato, A. Sakuma, and T. Miyazaki, Appl. Phys. Lett. **88**, 022503 (2006).

<sup>13</sup>A. Hütten, S. Kämmerer, J. Schmalhorst, A. Thomas, and G. Reiss, Phys. Status Solidi A **201**, 3271 (2004).

<sup>14</sup>W. F. Brinkman, R. C. Dynes, and J. M. Rowell, J. Appl. Phys. **41**, 1915 (1970).

<sup>15</sup>Y. Sakuraba, M. Hattori, M. Oogane, H. Kubota, Y. Ando, H. Kato, A. Sakuma, and T. Miyazaki, Appl. Phys. Lett. **88**, 192508 (2006).

<sup>16</sup>S. Yuasa, T. Nagahama, A. Fukushima, Y. Suzuki, and K. Ando, Nat. Mater. **3**, 868 (2004).

<sup>17</sup>Y. Ando, T. Miyakoshi, M. Oogane, H. Kubota, K. Ando, S. Yuasa, and T. Miyazaki, Appl. Phys. Lett. **87**, 142502 (2005).